Published in final edited form as:
J Biomed Mater Res A. 2014 May ; 102(5): 1527–1536. doi:10.1002/jbm.a.34829.

Effects of hyaluronic acid conjugation on anti-TNF-α inhibition of inflammation in burns

Emily E. Friedrich[1], **Liang Tso Sun**[1], **Shanmugasundaram Natesan**[2], **David O. Zamora**[2], **Robert J. Christy**[2], and **Newell R. Washburn**[1,3,4]

[1]Department of Biomedical Engineering, Carnegie Mellon University, Pittsburgh, Pennsylvania, USA

[2]United States Army Institute for Surgical Research, Fort Sam Houston, Texas, USA

[3]Department of Chemistry, Carnegie Mellon University, Pittsburgh, Pennsylvania, USA

[4]McGowan Institute for Regenerative Medicine, University of Pittsburgh, Pittsburgh, Pennsylvania, USA

Abstract

Biomaterials capable of neutralizing specific cytokines could form the basis for treating a broad range of conditions characterized by intense, local inflammation. Severe burns, spanning partial- to full-thickness of the dermis, can result in complications due to acute inflammation that contributes to burn progression, and early mediation may be a key factor in rescuing thermally injured tissue from secondary necrosis in order to improve healing outcomes. In this work we examined the effects on burn progression and influence on the inflammatory microenvironment of topical application of anti-TNF-α alone, mixed with hyaluronic acid or conjugated to hyaluronic acid. We found that non-conjugated anti-TNF-α decreased macrophage infiltration to a greater extent than that conjugated to hyaluronic acid; however there was little effect on the degree of progression or IL-1β levels. A simple transport model is proposed to analyze the results, which predicts qualitative and quantitative differences between untreated burn sites and those treated with the conjugates. Our results indicate that conjugation of anti-TNF-α to high molecular weight hyaluronic acid provides sustained, local modulation of the post-injury inflammatory responses compared to direct administration of non-conjugated antibodies.

Introduction

Conjugation of monoclonal antibodies against pro-inflammatory cytokines to high molecular weight hyaluronic acid (HA) has been shown to preserve antibody binding affinity[1] and lead to decreases in inflammatory responses in an incisional wound model.[2] It is hypothesized that the conjugates function by retarding cytokine diffusion in the extracellular environment, modulating the intensity of inflammatory responses through slowing the signaling cascade.[3]

Reprint requests: Newell R. Washburn, PhD, washburn@andrew.cmu.edu.

NRW has started a company to commercialize aspects of this research and discloses a potential conflict of interest.

Clinical application of this biomaterial would likely be in treating conditions characterized by intense inflammatory responses that worsen healing outcomes.

Burn injuries represent a potential clinical application of the conjugates due to intense inflammatory responses that can result in secondary tissue necrosis.[4] Severe burns that are partial to full thickness in depth can result in hypertrophic scarring, massive fluid shifts, sepsis and multi-organ failure.[5, 6] The initial burn results in necrosis immediately in what is known as the zone of coagulation but can progress over time into what is known as the zone of stasis.[7] This secondary necrosis may be due to inflammation-mediated mechanisms causing burn wound depth and surface area to progress for a period of up to 2 weeks after the initial injury.[8]

Hemostasis, inflammation, proliferation and remodeling are the four major phases of wound healing. These phases are distinct but overlapping, and sustained acute inflammation can inhibit the proliferation phase of wound healing, retarding the healing process. Acute inflammation is characterized by increases in pro-inflammatory cytokines, phagocytic macrophages and monocytes in the wound microenvironment, and blood vessel dilation and permeability. During acute inflammation, cytokines activate macrophages and monocytes which phagocytize dead cells, debris and the barrage of incoming microbial insults.[9] Tumor necrosis factor-α (TNF-α) is released by these activated macrophages, which remain activated due to their environment and the presence of other cytokines.[10] TNF-α is an upstream regulator of inflammation with a variety of potent effects, has been observed at significant levels in burn wound tissue and wound fluid[11] and therefore, is a key player in the destruction of tissue in burn wound progression. TNF-α causes dilation of blood vessels and enhances neutrophil adhesiveness to endothelium, which allows for both fluid shifts and for phagocytic white blood cells to enter the site of injury.[12] Neutrophils can block blood flow to tissue completely from excessive adherence to endothelium.[13] TNF-α may prolong neutrophil lifespan, leading to destruction of blood vessels by reactive oxygen species, heightening fluid shifts from blood to tissue.[14] Elevated levels of TNF-α induce keratinocytes, which are needed to repopulate the epidermis, to undergo apoptosis, further stalling the healing process.[15] A number of studies indicate that TNF-α is not strongly upregulated in serum post burn,[16, 17] however it has been found to be locally upregulated in burned skin,[11] therefore, local, controlled modulation of TNF-α signaling could result in broad improvements in healing outcomes due to its central role in inflammatory cascades at the wound site.

Currently on the market are antibody-based therapies that block TNF-α systemically in chronic inflammatory disease, such as ulcerative colitis and rheumatoid arthritis.[18] For example, the anti-TNF-α drug infliximab, which is a chimeric anti-TNF-α monoclonal antibody containing a murine TNF-α binding region and human IgG1 backbone has been shown to decrease symptoms of several inflammatory diseases.[19] This drug, however, can increase risk of infection, tuberculosis, cancer, and even increase risk of other inflammatory diseases such as psoriasis.[20] Many inflammatory conditions have a predominantly local manifestation, and to minimize side effects and increase effectiveness of anti-TNF-α treatment, we aim to modify the antibody to mediate inflammation locally, making it suitable for use in wound healing.

HA has been used in wound dressings, skin substitute products and other regenerative medicine applications.[21] A major constituent of the subepidermal glycosaminoglycans, HA is known to be both biocompatible and bioactive in wound healing. High molecular weight HA is diverse in function, having been shown to support migration, proliferation and cytokine production of fibroblasts, as well as immunosuppressive effects and radical scavenging properties.[22]

We previously described the biological activity of antibody-polymer conjugates.[2] In our most recent publication, we demonstrated that anti-TNF-α conjugated to HA was effective at reducing burn progression when compared to HA conjugated to anti-interleukin-6 or HA alone[23]. We also demonstrated that there were concomitant reductions in CD68+ cells and IL-1β production at sites treated with anti-TNF-α conjugated to HA. HA alone had a modest effect on dampening the development of nonviable tissue, but as far as IL-1β tissue levels and CD68+ cells, HA performed similarly to saline control. In the present study, we compared the effectiveness of the (anti-TNF-α)-HA conjugates to non-conjugated anti-TNF-α antibody and a non-conjugated mixture of HA and anti-TNF-α (anti-TNF-α + HA), in order to further elucidate the benefits of a topical antibody treatment that is designed to remain in the wound site for longer than a freely diffusing antibody.

MATERIALS AND METHODS

Materials

Hyaluronic acid (HA, M_w = 1.6 MDa) and 4-(dimethylamino) pyridine (4-DMAP) were purchased from Sigma-Aldrich (St. Louis, MO) and used as received. *N*-hydroxysulfosuccinimide sodium salt (sulfo-NHS) and *N*-(3-dimethylaminopropyl)-*N*-′-ethylcarbodiimide hydrochloride (EDC) were purchased from Pierce (Rockford, IL). Antir-TNF-α purified mouse monoclonal IgG, was purchased from R&D Systems, Inc. (Minneapolis, MN). All reagents were reconstituted and stored according to the manufacturer's instructions.

Monoclonal antibody conjugation to HA

Antibodies were conjugated to HA and characterized based on standard methods developed previously in our lab.[1] HA (12 mg) was modified with an active ester group, using Sulfo-NHS, EDC and 4-DMAP overnight, precipitated in acetone, and dried. Activated and rehydrated HA was coupled with anti-rTNF-α (1 mg), as shown in figure 1, at 4 °C overnight. The product was dialyzed (MW cut-off 300 kDa, Next Group, Southborough, MA) against PBS for 24 hours with 4 changes of PBS at 4 °C. The final product consisted of roughly 1% (w/v) HA solution. To achieve a higher viscosity more suitable for open wound applications, conjugate solution was made to contain 5% HA by mixing 3 parts of the conjugate product with 4 parts of 8% HA solution, and the final concentration of the cytokine-neutralizing antibody is about 400 μg/mL.

Binding affinity measurements

Binding affinity was determined based on methods previously described by our laboratory[1] using the ForteBio Octet QK system, which measures optical thickness of a streptavidin-

functionalized sensor tip. Antibodies, both modified and unmodified by HA conjugation, were biotinylated using EZ link sulfo-NHS LC-LC-biotin, which binds strongly to the streptavidin tip. Steptavidin sensor tips were hydrated in PBS for at least 5 minutes prior to starting the experiment. The experimental parameters consisted of the following dipping sequence: PBS 1 min (baseline), anti-TNF-α or (anti-TNF-α)-HA (10 μg/mL antibody) 20 min (loading), biocytin (10 μg/mL) 3 min (quench), PBS 5 min (wash), PBS 5 min (baseline), recombinant rat TNF-α (R&D systems Inc, Minneapolis, MN) 20 min (association), PBS 60 min (dissociation). The association step used a series of 6 TNF-α dilutions. The association rate constants, dissociation rate constants, and equilibrium dissociation constants were determined by using the Fortebio data analysis program, which calculated these values by generating a line of best-fit for the binding isotherm.

Rat deep partial-thickness burn model

A commercially available soldering unit was used as a controlled heat source. The soldering iron was modified by welding a 17 mm diameter, 2.5 mm thick brass disk on the tip and weighted with 500 g for efficient heat transfer. The non-contacting side of the disc was connected to a thermal coupler to monitor the actual temperature of the disk. All animal experiments were performed following the policies and procedures of the Institutional Animal Care and Use Committee at Institute of Surgical Research, Fort Sam Houston, TX. Burn injuries were induced on the back of 16 shaved, anesthetized adult Sprague-Dawley rats (n=4 for each treatment group). The brass disc was heated to 85 °C and stabilized for 2 min. One burn injury per rat was inflicted by placing the brass disc on the skin for 10 s. Eschar was excised the next day with surgical scissors, taking care to make the incision as close to the edge of the eschar as possible.[24] This was followed by application of 200 μL treatments. The treatment groups were saline, anti-TNF-α alone, anti-TNF-α mixed with HA (anti-TNF-α + HA) and (anti-TNF-α)-HA. The rats were randomized for different treatments and different time points. Eschar removal date was defined as day 0, and the first treatments were applied on the same day. The wounds were dressed with commercially available Tegaderm™ and sealed with Vetbond (3M, St. Paul, MN). Figure 2 provides a timeline for the burn study. Treatments were applied on days 0, 2 and 4, and the rats were euthanized and tissues around the burn were harvested on the days in which they were assigned. The tissue was prepared with either 10% formaldehyde for histology analysis or flash frozen for subsequent protein extraction.

Total protein and ELISA assays from burn tissue

The flash frozen tissues were cut into approximately 0.1 g pieces which were then homogenized in 600 μL of T-PER Tissue Protein Extraction solution (Thermo Scientific, Rockford, Illinois), for total protein extraction. Homogenates were centrifuged at 10,000 rcf for 5 min; supernatant was removed and stored at −80 °C.

The supernatants were assayed for total protein concentrations using the Pierce BCA Protein Assay kit (Thermo Scientific, Rockford, Illinois). The assay was carried out according to the kit procedure, with a 1:8 ratio of diluted sample to BCA working reagent and was analyzed by SAFIRE microplate reader (SAFIRE, San Jose, CA) with absorbance set at 562 nm. ELISA assays for IL-1β concentrations, from tissue extracts diluted 1:20 in assay diluent,

were performed using the Quantikine Rat IL-1β ELISA kit (R&D Systems, Minneapolis, MN), according to the kit procedures, and analyzed by SAFIRE microplate reader with absorbance 562 nm with a 549 nm correction. Curve fitting to the standards was used to express the concentration of both total protein and cytokines in the tissue samples in pg/mg protein.

Histological and immunohistochemical staining

Histological staining—The explanted burn site specimens mounted on glass slides and embedded in paraffin, were subsequently deparaffinized with xylene followed by a graded series of ethanol solutions (100–70%). Sections were then stained for hemotoxylin and eosin or Masson's Trichrome for morphological assessment. The slides were then cleared and dehydrated using the reverse of the deparaffinization procedure described above prior to coverslip with non-aqueous mount.

Immunohistochemical staining—Slides were stained for either vimentin, to determine the degree of viable tissue at the wound edge and apex, or for CD68, to approximate the number of macrophages infiltrating the wound bed deeper in the tissue along the axis of the wound edges. Following deparaffinization, the slides were immersed in 95–100 °C citrate antigen retrieval buffer (10 mM citric acid monohydrate, pH 6.0, Spectrum, Gardena, CA) for 20 min and cooled to 60 °C. Slides were washed twice in TRIS-buffered saline-Tween 20 (Trizma Base, Tween 20, Sigma) and twice in PBS. Tissue sections were incubated in T20 blocking buffer (Pierce, Rockford, IL) for 1 h at room temperature in a humidified chamber. Sections were incubated in primary antibody overnight at 4 °C in a humidified chamber, washed three times in PBS, then incubated in 3% H_2O_2 in methanol for 20 min at room temperature to quench endogenous peroxidase activity. Slides were washed three times in PBS before incubation in secondary antibody, biotinylated horse anti-mouse IgG (Vector, Burlingame, CA), for 1 hour in a humidified chamber at room temperature, and washed three times in PBS. The sections were then incubated in Vectastain ABC (Elite ABC kit, Vector) reagent for 30 min in a humidified 37 °C chamber, washed three times in PBS, and incubated in 4% diaminobenzadine substrate solution (DAB substrate peroxide kit, Vector) at room temperature. The slides were rinsed in water to stop the development of the diaminobenzadine substrate and counterstained using Harris hematoxylin stain (Vector). Slides were dehydrated using the reverse of the deparaffinization treatment described above prior to coverslipping. Primary antibodies used were mouse anti-rat CD68 (Serotec, Raleigh, NC), diluted to 1:100 in PBS or mouse anti-rat vimentin (Serotec, Raleigh, NC), diluted 1:20 in PBS. Secondary antibody was diluted in PBS 1:150 for CD68 staining, and 1:200 for vimentin staining. The immunostained slides were examined and imaged using a Leica DM IL LED microscope (Germany).

Statistical Analysis

Vimentin quantification, CD68 cell counts and IL-1β levels were all subjected to ANOVA to determine significance. IL-1β levels were log transformed for equal variance.

Results

Binding Affinity

Binding affinities were measured using the ForteBio Octet system, which uses heterodyne measurements of changes in the optical thickness at the ends of fiber optic sensors to measure the kinetics of adsorption and desorption. Binding affinity measurements were carried out on the antibody conjugate and the non-conjugated antibody. Association and dissociation curves are fit to equations of the following form:

$$R(t)=R_0+\Delta R(1-\exp[-k_{\text{on}}(t-t_{\text{on}})]) \quad (1)$$

$$R(t)=R_0+\Delta R\exp[-k_{\text{off}}(t-t_{\text{off}})] \quad (2)$$

where $R(t)$ is the reflection coefficient at time t, R_0 is the baseline value of the reflection coefficient, ΔR is the total change in response, k_{on} is the association rate constant, t_{on} is the time at which the sensor is placed in solution containing the analyte, k_{off} is the dissociation rate constant, and t_{off} is the time at which the sensor is placed in pure buffer solution. The values for k_{on} and k_{off} are determined from curve fitting, and their ratio provides a measurement of K_{D}.

Representative association and dissociation curves of (anti-TNF-α)-HA (figure 3a) and anti-TNF-α (figure 3b) are consistent with previous measurements from our lab. Differential initial loading of the biotinylated antibody, alone or as a conjugate, onto the streptavidin tip is observed, shown in figure 3c. The conjugate displays a greater thickness on the tip, perhaps due to interactions with HA chains.

Binding affinity for TNF-α by neutralizing mAb immobilized on the sensor tips was not significantly altered by conjugation to HA, with K_{D} values for both HA-conjugated and non-conjugated mAb around 100 pM. Previous studies by our lab confirmed this activity of the conjugates using in vitro measurements of NF-κB translocation assay[2], concluding that conjugation to high molecular weight HA does not abolish the affinity of mAb for TNF-α

Rat Burn experiment

Each rat received one burn and the next day, defined as day 0, the eschar was surgically removed before application of the treatments, as previously described by our lab.[25] Experimenters were blinded to the rat treatment groups. None of the rats lost a significant amount of weight during the experiments.

Qualitative histological assessment

As shown in figure 4, trichrome-stained tissue sections were analyzed qualitatively to determine gross appearance of the wound bed. Newly forming granulation tissue was observed in all cases by day 4, under both the intact skin and removed eschar; however wounds treated with the conjugate showed the most robust granulation tissue at this time point, which indicates that the (anti-TNF-α)-HA treatment group may be ahead temporally in terms of healing response compared to other treatment groups.

Although eschar was removed on day 1, newly forming eschar begins to appear in most treatment sites at days 4 and 7. This dark red layer is visibly thicker in the saline and non-conjugated anti-TNF-α treatments, which is postulated to be the result of secondary necrosis of the dermal tissue. This layer of tissue grew significantly in saline and anti-TNF-α treatments, shown on the day 7 images, but not in the (anti-TNF-α)-HA treatment group.

The viable tissue adjacent to the wound appears to remain healthiest in the (anti-TNF-α)-HA treatment group at day 7 compared to all other groups, maintaining epidermal and dermal structure. Hair follicles in this region appear intact in the (anti-TNF-α)-HA group, whereas in other treatment groups they appear damaged, especially in the saline control. Blood vessels in the tissue adjacent to the wound appear to be dilated one day after eschar removal in saline, and less so in anti-TNF-α, anti-TNF-α + HA and (anti-TNF-α)-HA treatments. This trend continues through day 7 for anti-TNF-α and (anti-TNF-α)-HA treatments show less dilation compared to saline treatments on day 1. Blood vessels from all treatment groups containing anti-TNF-α non-conjugated, mixed or conjugated, continue to trend towards dilation resistance through day 7 compared to saline treatment.

H&E staining revealed differences in the inflammatory immune response, as noted by immune cell infiltration by day 7 as shown in figure 5.

Multinucleated immune cells are prominent and densely packed at the wound edge. The density and thickness of this layer of immune cells evident in this area appears to decrease when comparing saline to anti-TNF-α and further decreases amongst the HA containing groups HA alone, anti-TNF-α + HA and (anti-TNF-α)-HA. In the (anti-TNF-α)-HA treatments, these areas of immune cells were less dense than observed in other treatment groups, suggesting an attenuation of the acute inflammatory response.

Vimentin immunostain quantification

Vimentin is an intermediate filament found in mesodermal tissues such as the dermis. Staining for vimentin is an established method of determining tissue viability,[26] and was used to identify burn progression after 7 days in this study. The extent of nonviable or significantly compromised tissue, which was identified with this stain as a lack of or extremely sparse staining for vimentin, is an estimate of burn progression. The vimentin-stained images were quantified in two separate rounds of blinded analysis, and the average thickness of the nonviable tissue was measured separately at each edge of the burn wound and in the center using ImageJ. A minimum of three images of each tissue section were examined at 4× magnification to measure this depth. These measurements were then averaged for the final results. The saline-treated control displayed the most nonviable tissue at day 7, as shown in figure 6. HA, anti-TNF-α and anti-TNF-α + HA treatments appeared to produce a relative decrease in nonviable tissue compared to saline by day 7, though not statistically significantly. (Anti-TNF-α)-HA treatment displayed the greatest decrease in nonviable tissue by day 7, which was significantly less than all other treatments ($p<0.003$).

Macrophage infiltration

Immunostaining for CD68 was used to assess the total number of active macrophages in the wound bed, inside the junction between healthy and damaged tissue about 200–500 μm

deep, depending on the day post wounding. The stained images were evaluated quantitatively in a blinded fashion by two independent investigators (MR and JP). Quantitative analysis was performed by counting the number of CD68 positive cells in three matched microscope fields at 40x magnification. The number of positive stained cells was then averaged to obtain the final results, as shown in figure 7. Treatment with anti-TNF-α or (anti-TNF-α)-HA significantly affected macrophage counts compared to saline (day 1, $p<0.001$; day 4, $p<0.05$; day 7, $p<.001$); anti-TNF-α +HA followed this pattern as well for later time points, but had no effect on day 1 (day 4, $p<.05$; day 7, $p<.001$). Treatment with (anti-TNF-α)-HA or anti-TNF-α +HA decreased the number of macrophages by day 7 compared to saline by nearly 20%. Anti-TNF-α treatment decreased the levels of macrophages the most by day 4 and day 7 compared to saline by approximately 75% and compared to (anti-TNF-α)-HA, about 50 percent. In reducing macrophage infiltration, treatment with non-conjugated anti-TNF-α appeared to have the largest effect, while (anti-TNF-α)-HA and anti-TNF-α + HA appeared to have similar effects on macrophage infiltration.

IL-1β concentrations

The cytokine IL-1β was chosen as a marker for the overall inflammatory microenvironment because it is centrally involved in inflammation and linked to the levels of active TNF-α,[16, 17] increasing to significant and measureable levels 1–3 hours after burn injury.[27, 28] As shown in figure 8, IL-1β levels were found to decrease the most in treated sites by anti-TNF-α on day 1, compared to saline though not significantly compared to the conjugate. Non-conjugated anti-TNF-α seemed to have the greatest effect early on in treated sites, but its efficacy decreased over time, and by day 7, anti-TNF-α treatment was similar to saline control. IL-1β levels were effectively reduced in (anti-TNF-α)-HA treated sites by day 4 and day 7, compared to saline (day 4, $p<.05$; day 7, $p<0.05$).

Discussion

Because of the demonstrated involvement of acute inflammation in aberrant burn healing,[7] modulation of inflammation is an appealing strategy for improving burn outcomes, but there are few documented studies on its effects. This may be because of the risks associated with systemic delivery of anti-inflammatory drugs to burn patients. The most effective and safest way to achieve this is through local therapy at the wound site. As we have shown, (anti-TNF-α)-HA, anti-TNF-α and anti-TNF-α + HA were all able to affect certain aspects of inflammation and healing through topical application of treatment, but the differences between their performances may be attributed to differences in pharmacokinetics of these therapeutics in the wound bed. In tissue, the diffusion coefficient of therapeutic antibodies is 10^{-8}–10^{-9} cm^2/s,[29] and mean residence time at the tissue is primarily determined by the diffusion time to a blood vessel, which would be of order 0.1 mm from the surface of rat epidermis,[30] from which a half-life on the order of hours would be predicted. In contrast, the high molecular weight of HA would cause tethered antibody to diffuse much slower, giving it an estimated diffusion coefficient in tissue of about 10^{-10} – 10^{-11} cm^2/s.[31] Based on diffusion constants, the conjugates would have a mean residence time on the order of days, although this will be reduced as the HA is degraded at the injury site by phagocytic cells and

reactive oxygen species. Given that HA has a half-life of about 50 h in subcutaneous tissue,[32] although likely less in a burn site, the residence time of the anti-TNF-α should be much greater when conjugated to high molecular weight HA. The increased residence time of (anti-TNF-α)-HA is hypothesized to reduce secondary necrosis significantly, which was most likely the combined result of decreasing IL-1β levels, general inflammatory cells at the wound front and active macrophages in the wound bed compared to saline. This was more effective than anti-TNF-α alone or anti-TNF-α + HA, which exhibited reduced macrophage counts, but did not significantly decrease the nonviable tissue or IL-1β compared to saline. Because the degree of nonviable tissue in anti-TNF-α and anti-TNF-α + HA treatment was much greater than in the (anti-TNF-α)-HA treatment, we postulate that the faster diffusion of non-conjugated anti-TNF-α through tissue was able both to inhibit recruitment of macrophages and possibly block TNF-α effects on blood vessel dilation more effectively due to antibody diffusion into the blood vessel. However, the spectrum of TNF-α activities at the wound site went unhindered, as seen by the robust recruitment of immune cells under newly forming eschar on days 4 and 7.

Although non-conjugated antibody was initially effective in decreasing IL-1β levels at day 1 compared to saline control and conjugate, and in decreasing macrophage counts throughout, we hypothesize that the antibody diffuses rapidly from the wound site and into the blood stream too quickly to provide a sustained decrease in inflammation at the site over a long period of time in the pivotal zone of stasis. It is interesting that under treatment with anti-TNF-α, the measured macrophage numbers and IL-1β concentrations appear to be anti-correlated: macrophage numbers are relatively higher at Day 1 and lower at Day 4 and Day 7 while the opposite trend is observed in IL-1β levels. We propose that other resident or recruited immune cells may be responsible for the observed IL-1β levels, but follow-up studies are required to determine this.

A simple transport model may be used to interpret the reductions in inflammatory markers under treatment with conjugated anti-TNF-α compared to non-conjugated using standard transport equations[33]

$$\partial c_{TNF}/\partial t = \overline{v} \cdot \nabla c_{TNF} + D\partial^2 c_{TNF}/\partial r^2 + \square \quad (3)$$

where c_{TNF} represents the local concentration of TNF-α as a function of position r and time t, the first term on the right (assumed to be zero) represents transport due to convection involving the dot product of a velocity v with the gradient of c_{TNF}, D is the effective diffusion constant of TNF-α in the tissue having value of 2×10^{-7} cm^2/s,[34] and Γ is the volumetric production rate of TNF-α. Production of TNF-α in burned rodent skin increases significantly compared to baseline levels in healthy skin,[11] with levels reported of roughly 1500 ± 300 pg/(μg soluble protein) compared to negligible TNF-α levels in healthy skin 3 days following partial-thickness burns. Direct measurements of TNF-α concentrations were not successful in antibody-treated sites in our study, potentially due to the confounding effects of TNF-α antibodies. A volumetric production rate of 15 μg/mL·day in the zone of stasis was estimated, based on calculations with reported TNF-α values in burned rodent skin, and we assume further that the surrounding zone of stasis produces TNF-α at a rate

that maintains a boundary condition of $\partial c_{TNF}/\partial z = 0$ at the interface between zones. If the antibody conjugate is restricted to the outer layer of the burn site, it can be assumed to form a sink for TNF-α at which $c_{TNF}(z=0) = 0$ since the amount of mAb applied (100 μg or 7×10^{-10} mol) is comparable to the number of moles of TNF-α produced in one day. If the zone of stasis in the burn sites is a cylindrical volume with diameter d = 17 mm and depth L = 3 mm, this model can be simplified as a one-dimensional diffusion equation that predicts a flux at the interface with the gel, a z-dependence, and an average TNF surface flux of

$$\square D\left(\square c_{TNF}\Big/_{\square z}\right)=\square\square L=4.5\mu\mathrm{g/cm}^2\cdot\mathrm{day} \quad (4)$$

which is the rate at which TNF is sequestered by the antibody conjugate. The concentration averaged over the volume of the burn site in the absence of the conjugate is predicted to increase linearly with time at a rate of $\Gamma^*\pi Ld^2$. However, in the presence of the conjugate, this is predicted to plateau at a value given by

$$\Gamma L^2/3D=26\mu\mathrm{g/mL} \quad (5)$$

until the antibody sites are filled. In analyzing the model, we did not explicitly consider the effects of reversible binding of TNF-α by the antibody or the effects of antibody saturation. Interestingly, increasing antibody dose only affects TNF-α concentrations beyond the saturation limit, and in these experiments the dose is just enough to capture TNF-α produced in the first 48 hours. The results of this model suggest that significant shifts in TNF-α concentration and transport can be effected through application of the antibody-polymer conjugates, and further refinement of the model could result in more insight into these processes.

Current theories suggest multiple macrophage phenotypes are involved in wound healing, and this phenotype evolves over the course of productive healing.[35] Tethering the antibody to biopolymer may be more effective in two ways: by keeping the antibody physically in the wound for longer without diffusion into the bloodstream, and by sterically blocking the Fc region of the antibody, a major contributor to innate immune responses to therapeutic antibodies. The latter is important to the mode of inhibition of TNF-α. Macrophages can have TNF-α on their surface, to which non-conjugated antibody can bind.[36] This tags the macrophage for removal and/or cell death which could account for the dramatic decrease in macrophage count in the anti-TNF-α treatment group. It is also possible that non-conjugated anti-TNF-α moving into the blood stream inhibits further recruitment of circulating monocytes. Because nonviable tissue was not decreased in this treatment despite the decrease in macrophage count, this may indicate that despite reducing macrophage numbers, the remaining cells are still highly active in the wound site. Considering the plasticity of macrophages involved in wound healing, significantly reducing the macrophages could have a negative effect on healing; the same macrophages needed to phagocytize debris are needed to initiate the repair processes.[37,38] Further experiments on mechanisms of cell death will be needed to explore this concept.

HA has been shown to have anti-inflammatory properties in burn wound healing.[39] While we did see a small decrease in nonviable tissue with HA alone[23], HA did not significantly

affect the biochemical markers of inflammation that we wish to modulate during the pivotal early stages of wound healing. Conjugated to anti-TNF-α though, we were able to decrease nonviable tissue and the related inflammatory markers more effectively than with anti-TNF-α, HA or anti-TNF-α + HA. We have yet to uncover the mechanism by which conjugation of the antibody to HA was able to decrease the inflammatory response and burn progression compared to merely a mixture of the two components. This will be further investigated in a study comparing conjugation of the antibody to various polysaccharides with different biological inertness or activity. High levels of TNF-α are associated with pathologies in wound healing, and localization of the capturing antibody is key to decreasing the amount of nonviable tissue that results.

Acknowledgments

The authors acknowledge support from the Armed Forces Institute of Regenerative Medicine (W81XWH-08-2-0032) and the National Institutes of Health (R43GM085897). NRW gratefully acknowledges support from a 3M Non-Tenured Faculty Grant, the Wallace H. Coulter Foundation Translational Research Award program, and the Heinz Endowment (C1747). The authors wish to thank John Walters for statistics and Rodrigo Perez-Segnini for help with graphics. The authors also wish to thank Dr. Yoram Vodovotz, Dr. Lillian Nanney and Dr. Todd Przybycien for helpful technical discussions.

Abbreviations

anti-TNF-α	anti-tumor necrosis factor-α
HA	hyaluronic acid
(anti-TNF-α)-HA	anti-tumor necrosis factor-α hyaluronic acid conjugate
IL-1β	interleukin-1β

References

1. Sun LT, Buchholz KS, Lotze MT, Washburn NR. Cytokine Binding by Polysaccharide-Antibody Conjugates. Mol Pharm. 2010
2. Sun LT, Bencherif SA, Gilbert TW, Farkas AM, Lotze MT, Washburn NR. Biological activities of cytokine-neutralizing hyaluronic acid-antibody conjugates. Wound Repair Regen. 2010; 18(3):302–310. [PubMed: 20412551]
3. Sun LT, Bencherif SA, Gilbert TW, Lotze MT, Washburn NR. Design principles for cytokine-neutralizing gels: Cross-linking effects. Acta Biomater. 2010; 6(12):4708–4715. [PubMed: 20601239]
4. Jackson DM. The diagnosis of the depth of burning. Br J Surg. 1953; 40:588–596. [PubMed: 13059343]
5. Johnson RM, Richard R. Partial-thickness burns: identification and management. Adv Skin Wound Care. 2003; 16(4):178–187. quiz 88–9. [PubMed: 12897674]
6. Singh V, Devgan L, Bhat S, Milner SM. The pathogenesis of burn wound conversion. Ann Plast Surg. 2007; 59(1):109–115. [PubMed: 17589272]
7. Shupp JW, Nasabzadeh TJ, Rosenthal DS, Jordan MH, Fidler P, Jeng JC. A review of the local pathophysiologic bases of burn wound progression. J Burn Care Res. 2010; 31(6):849–873. [PubMed: 21105319]
8. Arturson G. Pathophysiology of the burn wound and pharmacological treatment. The Rudi Hermans Lecture, 1995. Burns. 1996; 22(4):255–274. [PubMed: 8781717]
9. Akira S, Takeda K. Toll-like receptor signalling. Nat Rev Immunol. 2004; 4(7):499–511. [PubMed: 15229469]

10. Beutler B, Cerami A. The biology of cachectin/TNF--a primary mediator of the host response. Annu Rev Immunol. 1989; 7:625–655. [PubMed: 2540776]
11. Schwacha MG, Thobe BM, Daniel T, Hubbard WJ. Impact of thermal injury on wound infiltration and the dermal inflammatory response. J Surg Res. 2010; 158(1):112–120. [PubMed: 19394637]
12. Zhang C, Wu J, Xu X, Potter BJ, Gao X. Direct relationship between levels of TNF-alpha expression and endothelial dysfunction in reperfusion injury. Basic Res Cardiol. 2010; 105(4): 453–464. [PubMed: 20091314]
13. Proudman SM, Cleland LG, Mayrhofer G. Effects of tumor necrosis factor-alpha, interleukin 1beta, and activated peripheral blood mononuclear cells on the expression of adhesion molecules and recruitment of leukocytes in rheumatoid synovial xenografts in SCID mice. J Rheumatol. 1999; 26(9):1877–1889. [PubMed: 10493665]
14. Edwards SW, Derouet M, Howse M, Moots RJ. Regulation of neutrophil apoptosis by Mcl-1. Biochem Soc Trans. 2004; 32(Pt3):489–492. [PubMed: 15157168]
15. Piguet PF, Grau GE, Vassalli P. Subcutaneous perfusion of tumor necrosis factor induces local proliferation of fibroblasts, capillaries, and epidermal cells, or massive tissue necrosis. Am J Pathol. 1990; 136(1):103–110. [PubMed: 1688687]
16. Finnerty CC, Przkora R, Herndon DN, Jeschke MG. Cytokine expression profile over time in burned mice. Cytokine. 2009; 45(1):20–25. [PubMed: 19019696]
17. Finnerty CC, Herndon DN, Przkora R, Pereira CT, Oliveira HM, Queiroz DM, Rocha AM, Jeschke MG. Cytokine expression profile over time in severely burned pediatric patients. Shock. 2006; 26(1):13–19. [PubMed: 16783192]
18. Sfikakis PP. The first decade of biologic TNF antagonists in clinical practice: lessons learned, unresolved issues and future directions. Curr Dir Autoimmun. 2010; 11:180–210. [PubMed: 20173395]
19. Gupta AK, Skinner AR. A review of the use of infliximab to manage cutaneous dermatoses. J Cutan Med Surg. 2004; 8(2):77–89. [PubMed: 15685387]
20. Scheinfeld N. A comprehensive review and evaluation of the side effects of the tumor necrosis factor alpha blockers etanercept, infliximab and adalimumab. J Dermatolog Treat. 2004; 15(5): 280–294. [PubMed: 15370396]
21. Voigt J, Driver VR. Hyaluronic acid derivatives and their healing effect on burns, epithelial surgical wounds, and chronic wounds: a systematic review and meta-analysis of randomized controlled trials. Wound Repair Regen. 2012; 20(3):317–331. [PubMed: 22564227]
22. Salbach J, Rachner TD, Rauner M, Hempel U, Anderegg U, Franz S, Simon JC, Hofbauer LC. Regenerative potential of glycosaminoglycans for skin and bone. J Mol Med (Berl). 2012; 90(6): 625–635. [PubMed: 22187113]
23. Sun LT, Friedrich E, Heuslein JL, Pferdehirt RE, Dangelo NM, Natesan S, Christy RJ, Washburn NR. Reduction of burn progression with topical delivery of (antitumor necrosis factor-alpha)-hyaluronic acid conjugates. Wound Repair Regen. 2012; 20(4):563–572. [PubMed: 22712482]
24. Chang KC, Ma H, Liao WC, Lee CK, Lin CY, Chen CC. The optimal time for early burn wound excision to reduce pro-inflammatory cytokine production in a murine burn injury model. Burns. 2010; 36(7):1059–1066. [PubMed: 20471756]
25. Liang Tso Sun EF, Heuslein Joshua L, Pferdehirt Rachel E, Dangelo Nicole M, Natesan Shanmugasundaram, Christy Robert J, Washburn Newell R. Reduction of burn progression with topical delivery of (anti-tumor necrosis factor-α)-hyaluronic acid conjugates. Wound Repair and Regeneration. 2012
26. Nanney LB, Wenczak BA, Lynch JB. Progressive burn injury documented with vimentin immunostaining. J Burn Care Rehabil. 1996; 17(3):191–198. [PubMed: 8736363]
27. Gauglitz GG, Song J, Herndon DN, Finnerty CC, Boehning D, Barral JM, Jeschke MG. Characterization of the inflammatory response during acute and post-acute phases after severe burn. Shock. 2008; 30(5):503–507. [PubMed: 18391855]
28. Sakallioglu AE, Basaran O, Karakayali H, Ozdemir BH, Yucel M, Arat Z, Haberal M. Interactions of systemic immune response and local wound healing in different burn depths: an experimental study on rats. J Burn Care Res. 2006; 27(3):357–366. [PubMed: 16679907]

29. Clauss MA, Jain RK. Interstitial transport of rabbit and sheep antibodies in normal and neoplastic tissues. Cancer Res. 1990; 50(12):3487–3492. [PubMed: 2340499]

30. Cevc G, Vierl U. Spatial distribution of cutaneous microvasculature and local drug clearance after drug application on the skin. J Control Release. 2007; 118(1):18–26. [PubMed: 17254662]

31. Kaminski T, Siebrasse JP, Gieselmann V, Kubitscheck U, Kappler J. Imaging and tracking of single hyaluronan molecules diffusing in solution. Glycoconj J. 2008; 25(6):555–560. [PubMed: 18259857]

32. Laurent UB, Fraser JR, Laurent TC. An experimental technique to study the turnover of concentrated hyaluronan in the anterior chamber of the rabbit. Exp Eye Res. 1988; 46(1):49–58. [PubMed: 3342833]

33. Cheong R, Bergmann A, Werner SL, Regal J, Hoffmann A, Levchenko A. Transient IkappaB kinase activity mediates temporal NF-kappaB dynamics in response to a wide range of tumor necrosis factor-alpha doses. J Biol Chem. 2006; 281(5):2945–2950. [PubMed: 16321974]

34. Francis K, Palsson BO. Effective intercellular communication distances are determined by the relative time constants for cyto/chemokine secretion and diffusion. Proc Natl Acad Sci U S A. 1997; 94(23):12258–12262. [PubMed: 9356436]

35. Daley JM, Brancato SK, Thomay AA, Reichner JS, Albina JE. The phenotype of murine wound macrophages. J Leukoc Biol. 2010; 87(1):59–67. [PubMed: 20052800]

36. Arend WP. The mode of action of cytokine inhibitors. J Rheumatol Suppl. 2002; 65:16–21. [PubMed: 12236617]

37. Duffield JS. The inflammatory macrophage: a story of Jekyll and Hyde. Clin Sci (Lond). 2003; 104(1):27–38. [PubMed: 12519085]

38. Juniantito V, Izawa T, Yamamoto E, Murai F, Kuwamura M, Yamate J. Heterogeneity of Macrophage Populations and Expression of Galectin-3 in Cutaneous Wound Healing in Rats. J Comp Pathol. 2011

39. Voinchet V, Vasseur P, Kern J. Efficacy and safety of hyaluronic acid in the management of acute wounds. Am J Clin Dermatol. 2006; 7(6):353–357. [PubMed: 17173469]

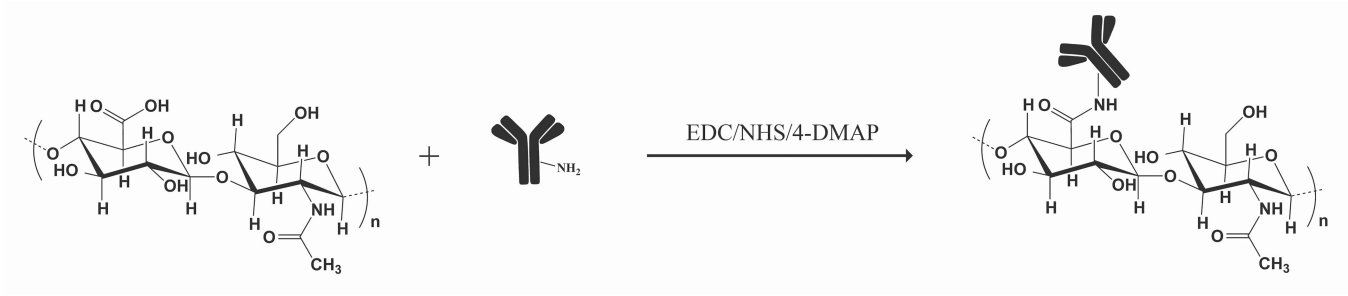

Figure 1.

a. Schematic of conjugation. HA was activated with EDC to form amide bond with an amine group on the antibody.

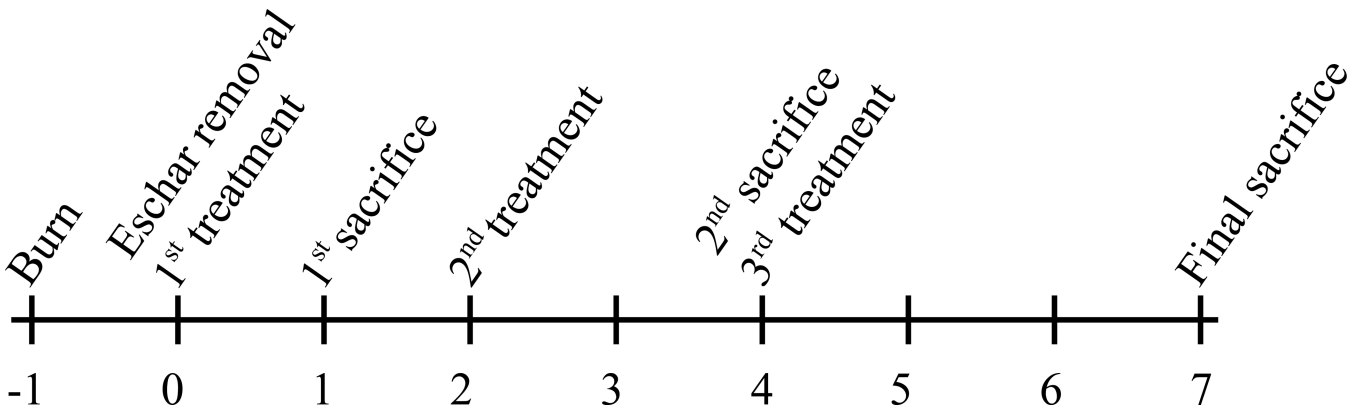

Figure 2.

Timeline of burn experiment. There were 3 time points, with n=4 animals receiving 1, 2 or 3 treatments over a course of 1, 4 or 7 days, respectively.

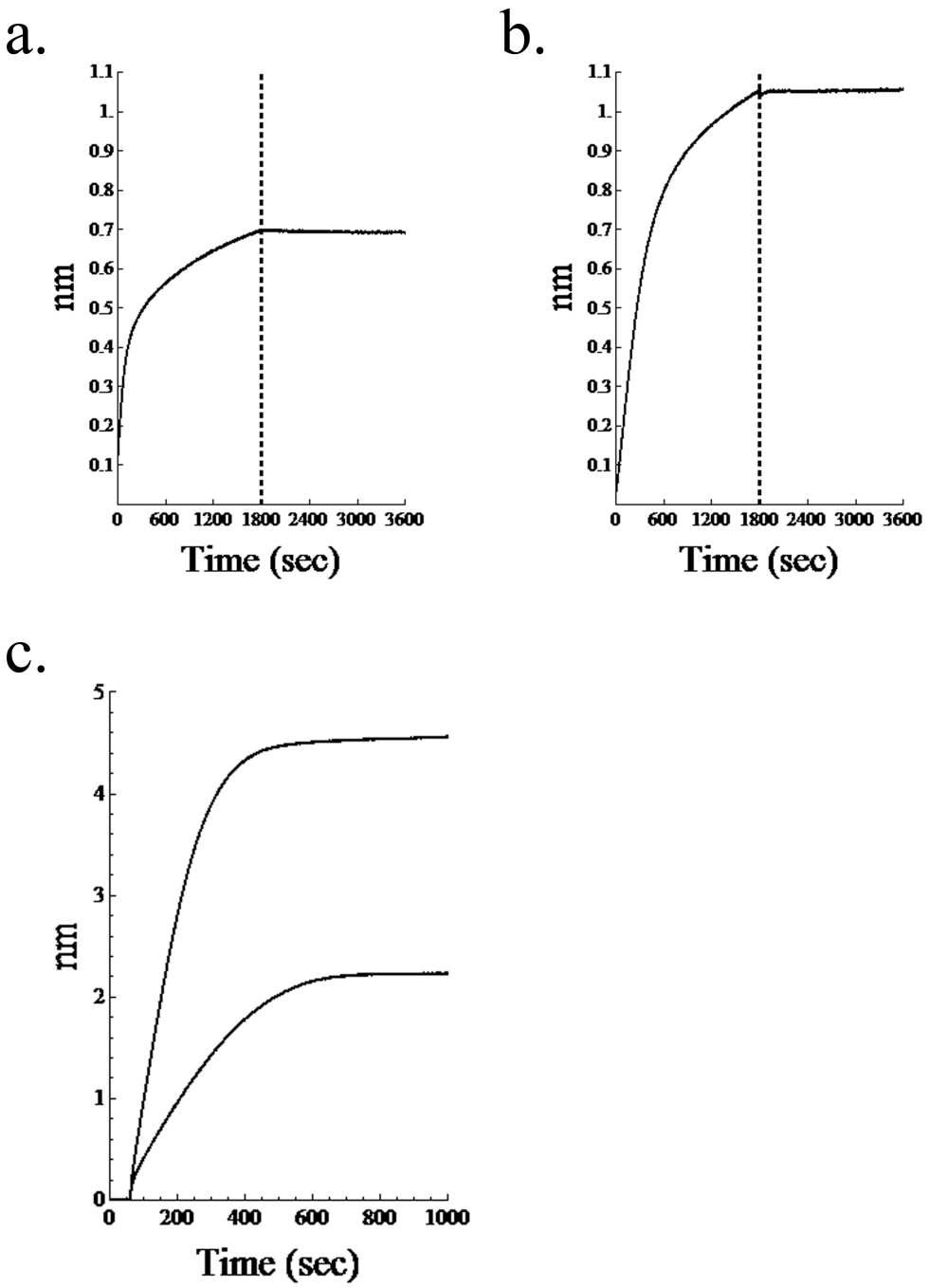

Figure 3.

Binding affinity experiments. Association and dissociation curves for (a.) (anti-TNF-α)-HA and (b.) anti-TNF-α. Vertical line separates association, on the left from dissociation. c. Comparison of initial loading of biotinylated antibody and conjugate onto streptavidin tips. Greater thickness is observed for the conjugate possibly due to interactions with HA chains.

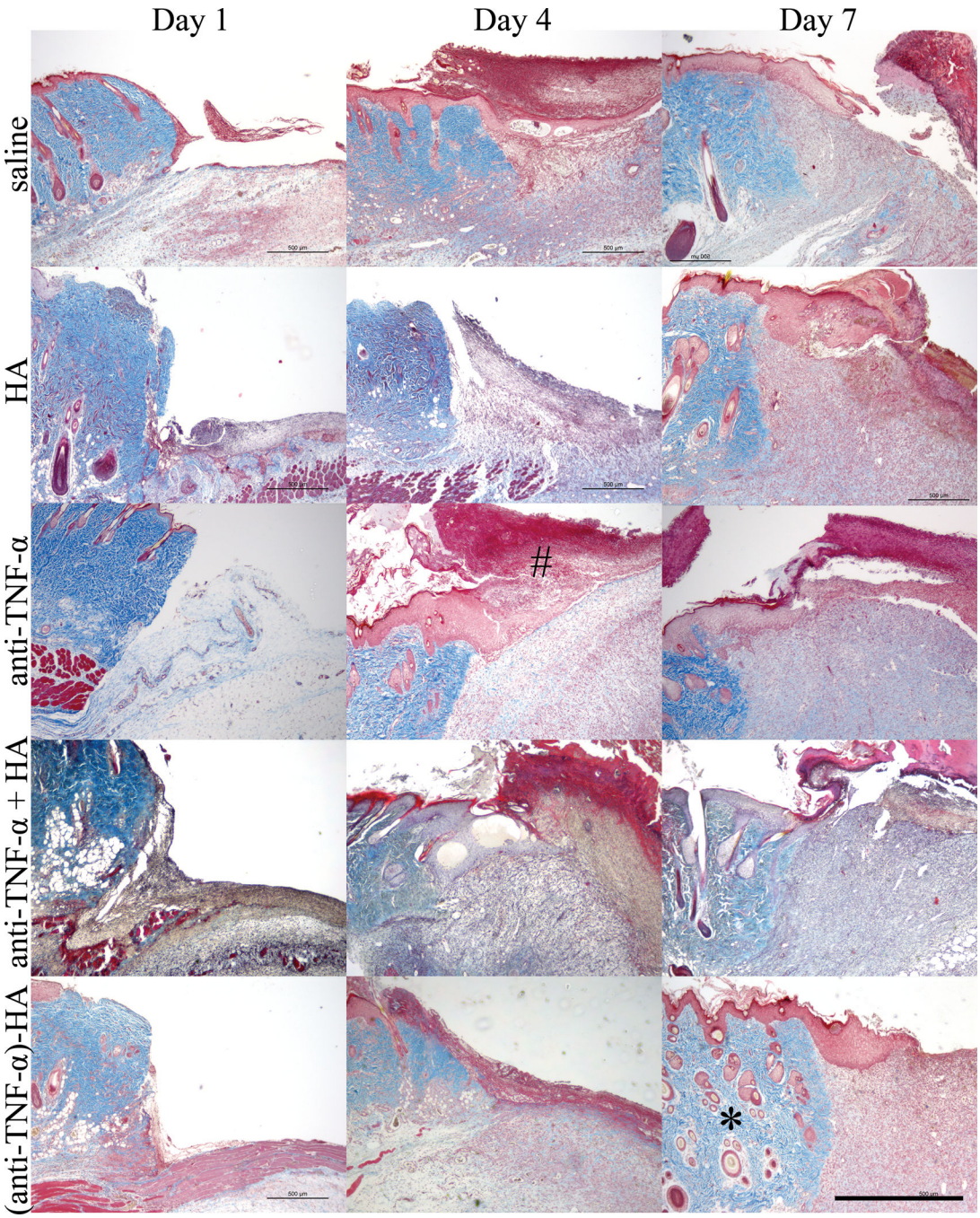

Figure 4.

Masson's trichrome images of burn edges. Granulation tissue started to appear four days after eschar removal in the deep dermal region, with the most robust granulation tissue in the (anti-TNF-α)-HA treated sites. HA, anti-TNF-α and anti-TNF-α + HA treatments shows slower granulation tissue formation, while saline treated wound sites display the slowest granulation tissue formation. On day 4, newly forming eschar (#) is observed in most of the wound sites, and on day 7, necrosis has grown significantly particularly in saline and anti-

TNF-α treated burn sites. Adjacent tissue (*) appears healthiest day 7 in the (anti-TNF-α)-HA treated sites. Scale bar = 1mm.

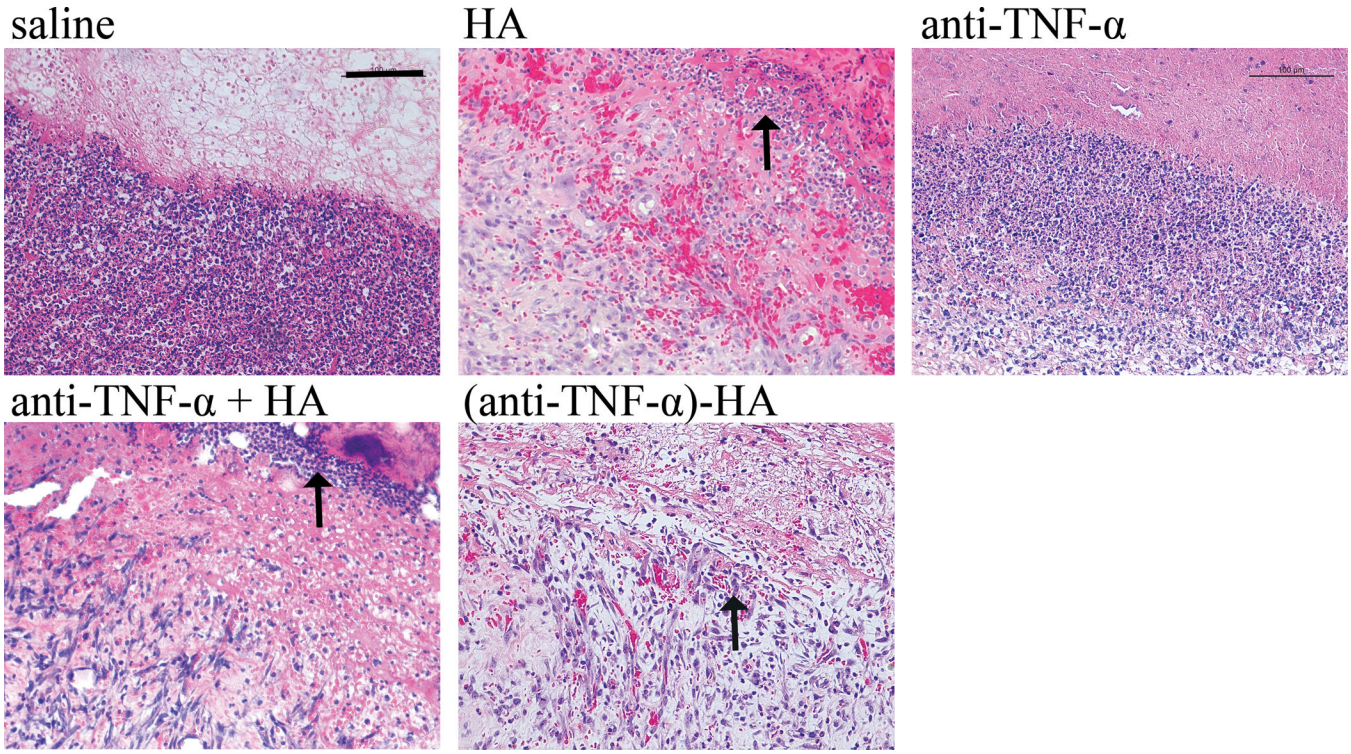

Figure 5.

H & E staining. Day 7 images of the burn at the interface of wound edge and newly formed eschar shows densely populated multinucleated inflammatory immune cells apparent in saline and anti-TNF-α treatments. These immune cells, indicated with an arrow, are less densely populated in HA and anti-TNF-α + HA, with the fewest and most sparse found with (anti-TNF-α)-HA treatments. Scale bar = 200 μm.

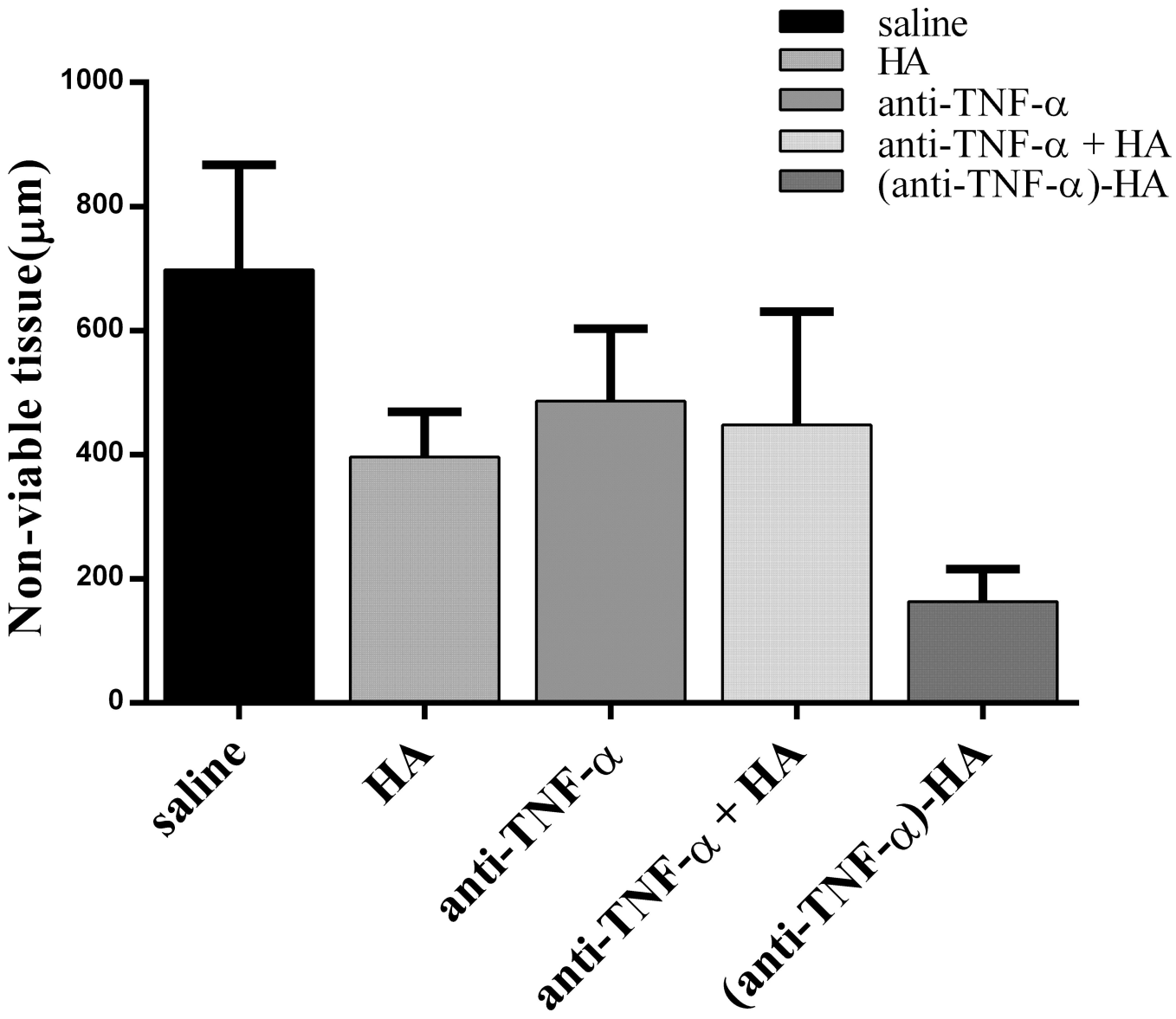

Figure 6.

Vimentin immunostaining was used to assess viable tissue, by measuring thickness of nonviable tissue. Trichrome images were referenced if it was not immediately clear where the viable tissue ended. By day 7, (anti-TNF-α)-HA has decreased the thickness of necrosis significantly. (Anti-TNF-α)-HA treated burn sites have significantly thinner nonviable zones than saline and anti-TNF-α treated sites and denser vimentin staining in the viable region. Thickness of nonviable tissue in anti-TNF-α treated sites is not significantly different from saline treatments, but trends towards a slight reduction in nonviable tissue. *: $p<0.05$; error bars = mean +/− SD

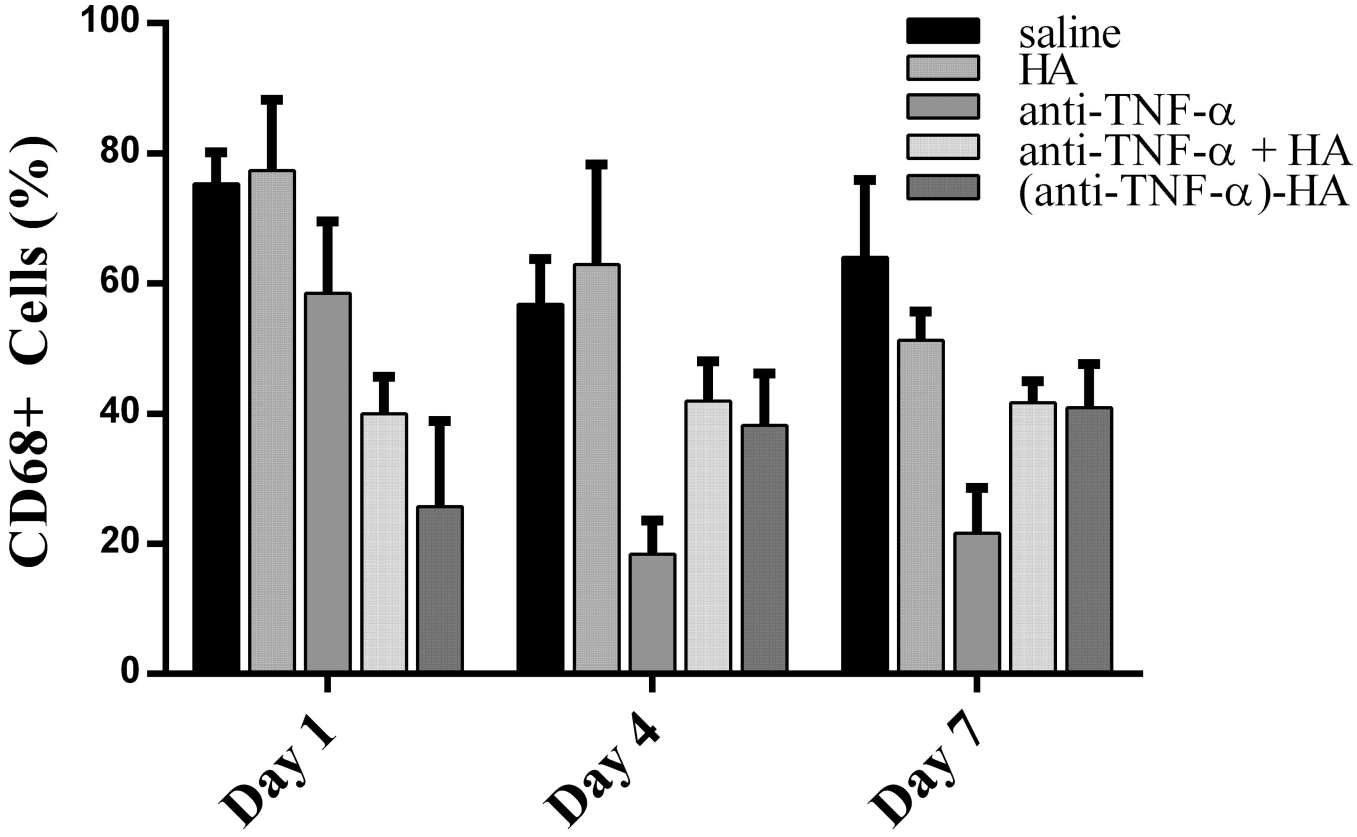

Figure 7.

Macrophage infiltration counts. On day 1, macrophage count appears to be most affected by (anti-TNF-α)-HA, and slightly by anti-TNF-α treatment. Anti-TNF-α treatments appeared to decrease macrophage counts the most by days 4 and 7. (Anti-TNF-α)-HA treatment attenuated slightly by day 7, but was still significantly decreased compared to saline control (* $p<.001$, bars $p<.05$; error bars are mean +/− SD).

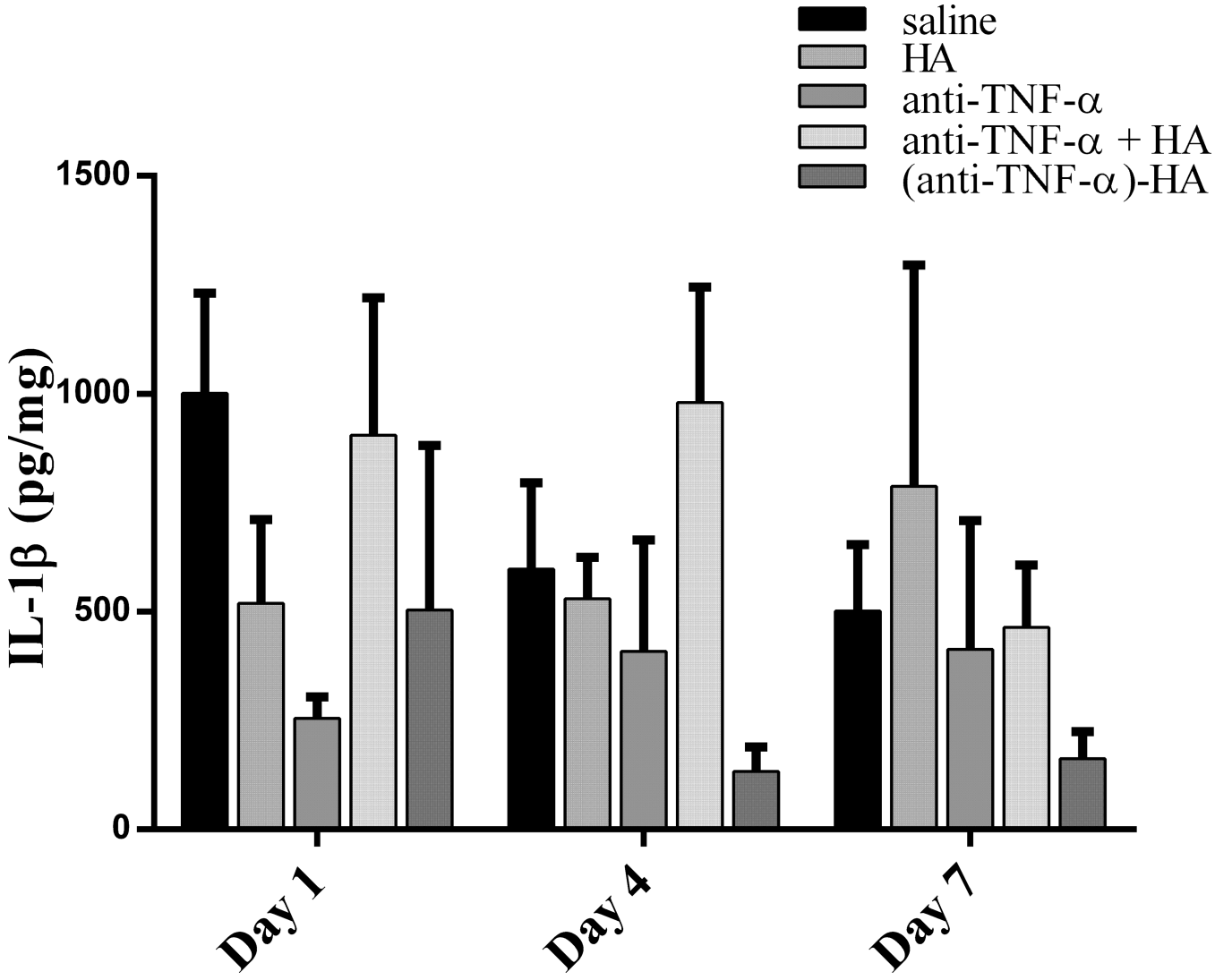

Figure 8.

IL-1β concentration in extracted burn tissue. IL-1β concentration peaks at day 1, and attenuates on day 4 in saline and (anti-TNF-α)-HA treated wound sites, however IL-1β levels are significantly lower than those in saline treated sites throughout the experimental period (* $p<0.01$ day 4, and $p<0.05$ day 7). Anti-TNF-α treatment exhibited the opposite response to saline and (anti-TNF-α)-HA, inhibiting IL-1β day 1 compared to saline, but then steadily loses effect by days 4 and 7. Error bars = mean +/− SD.

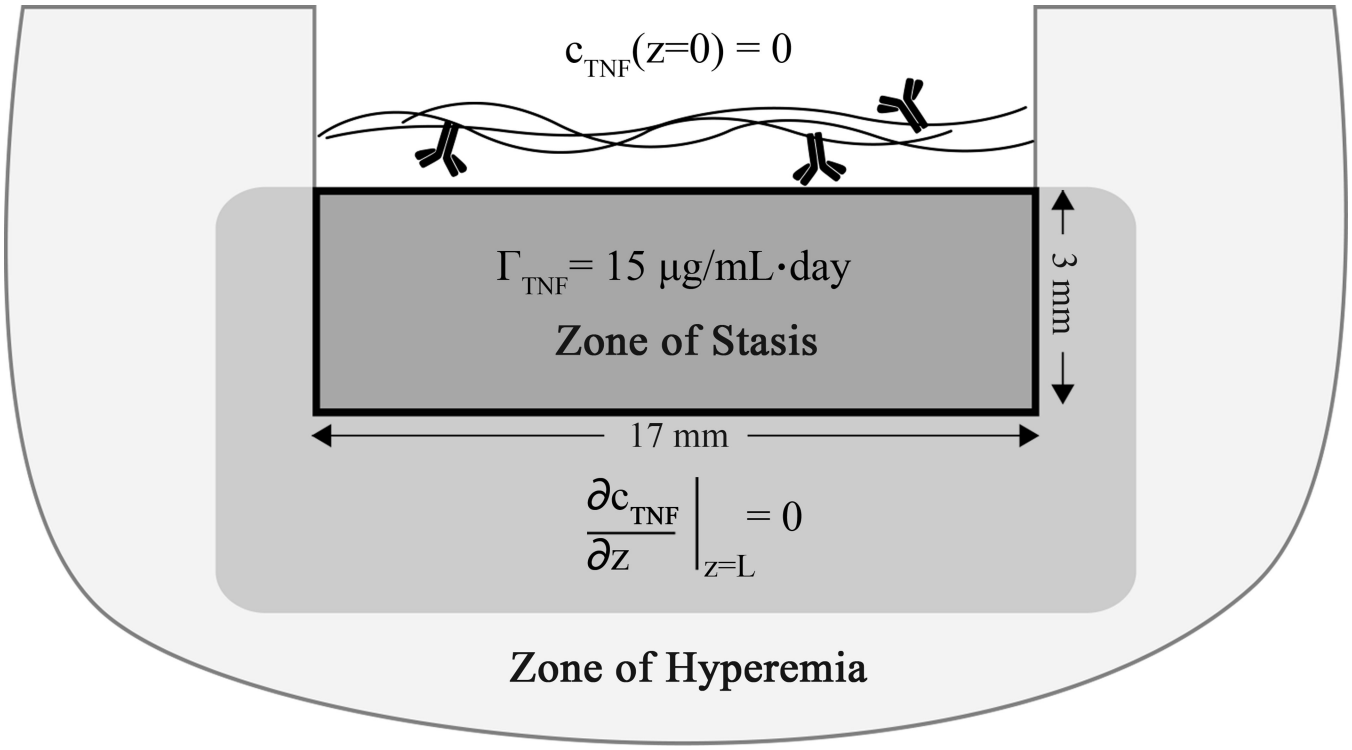

Figure 9.

Graphic representation of transport model. Total area represents a burn wound cross section. The solid black-bounded box represents the boundaries of the model, the contents of which also correlate to the zone of stasis, where the dramatic increases in TNF-α are expected to occur